Crystal-field-induced magnetic frustration in $NdMIn_5$ and Nd_2MIn_8 (M=Rh, Ir) antiferromagnets

P. G. Pagliuso, J. D. Thompson, M. F. Hundley, and J. L. Sarrao
Los Alamos National Laboratory, Los Alamos, New Mexico 87545
(Received 6 June 2000)

We have synthesized the series of compounds $NdMIn_5$ and Nd_2MIn_8 in single crystal form, where M = Rh or Ir. These materials form in tetragonal derivatives of the Cu_3Au-structure $NdIn_3$ compound. Measurements of magnetic susceptibility, electrical resistivity, and low-temperature heat capacity are reported. These compounds order antiferromagnetically at low temperature ($T_N < 14$ K) and the evolution of their magnetic properties depends on the crystal-field ground-state configuration. Comparison between the present data and magnetic properties of the isostrucutural new heavy fermion compounds $Ce(Rh,Ir)In_5$ and $Ce_2(Rh,Ir)In_8$ suggests that crystal field effects and magnetic anisotropy should be taken into account to understand the rich phase diagram of these compounds.

I. INTRODUCTION

Recently, a new series of $R_mM_nIn_{3m+2n}$ tetragonal variants of the Cu_3Au-structure compounds have been synthesized in single crystal form, for M=Rh or Ir, $m=1,2$; $n=1$ and R=La, Ce, Pr, Nd, Sm, and Gd.[1] Their tetragonal structure can be viewed as m layers of RIn_3 units stacked sequentially along the c axis with intervening n layers of MIn_2. The Ce-based compounds include a new class of heavy-fermion materials for which unconventional magnetic and superconducting behavior have been reported.[2–5] $CeRhIn_5$ is an antiferromagnet at ambient pressure with $T_N \approx 3.8$ K and an electronic specific heat $\gamma \approx 400$ mJ/mol K^2.[2] Pressure dependent electrical resistivity and specific heat experiments on $CeRhIn_5$ (Ref. 2) show an unconventionial evolution to a superconducting state for $P > P_c \approx 16$ kbar where superconductivity sets in at $T_c \approx 2.0$ K.

Another member of this family, $CeIrIn_5$, shows ambient-pressure bulk superconductivity at $T_c \approx 0.4$ K, inferred by a diamagnetic transition in the ac susceptibility coincident with a jump in heat capacity.[3,5] Just above T_c, C/T is essentially constant and gives a Sommerfeld coefficient of $\gamma \approx 720$ mJ/mole K^2.[3] The $n=2$ variants of these Ce-based compounds include an antiferromagnetic ground state ($T_N \approx 2.8$ K and $\gamma \approx 400$ mJ/mol K^2) for Ce_2RhIn_8, while Ce_2IrIn_8 remains a heavy-fermion paramagnet to 50 mK, with no evidence for a phase transition ($\gamma \approx 700$ mJ/mol K^2).[4]

It has been suggested that the reduced spatial dimensionality and magnetic anisotropy resulting from the quasi-2D structure of these compounds may control the nature of their heavy-fermion ground states.[2,4] Therefore, studies in non-Kondo isostructural magnetic materials of the same $R_mM_nIn_{3m+2n}$ series may be useful in understanding the role of spatial dimensionality, magnetic anisotropy, and crystal field effects (CEF) in the evolution of the magnetic properties within these series. As the Pr-based homologues are nonmagnetic singlet ground state systems,[1] the Nd-based materials are the obvious candidates for such a study.

Thus, we have performed magnetic susceptibility, electrical resistivity, and heat capacity measurements in $NdMIn_5$ and Nd_2MIn_8 single crystals, for M=Rh or Ir. Each orders antiferromagnetically with $T_N \lesssim 14$ K. Comparisons to their cubic relative $NdIn_3$ suggest that the symmetry of the crystal field ground state drives the evolution of the magnetic properties for the tetragonal variants. An analogous interpretation for the Ce-based materials is also discussed.

II. EXPERIMENT

Single crystalline samples of the $NdMIn_5$ and Nd_2MIn_8 (M=Rh or Ir) compounds were grown from the melt in In flux as described previously.[2] Typical crystal sizes were 1 cm×1 cm× several mm. The tetragonal $Ho_mCo_nGa_{3m+2n}$ ($m=1,2; n=1$) structure types and phase purity were confirmed by x-ray powder diffraction, and the crystal orientation was determined by the usual Laue method. The lattice parameters a and c for the studied compounds are given in Table I. Specific heat measurements were performed in a small-mass calorimeter system that employs a quasiadiabatic thermal relaxation technique.[6] Samples used here ranged from 10 to 30 mg. Magnetization measurements up to ≈5 kbar were made in a Quantum Design dc Superconducting Quantum Interference Device magnetometer using a small clamp-type cell with flourinert-75 as the pressure medium. Electrical resistivity was measured using a low-frequency ac resistance bridge and four-contact configuration.

TABLE I. Experimental parameters for $NdMIn_5$, Nd_2MIn_8 (M=Rh or Ir) and $NdIn_3$.

	a Å	c Å	V Å^3	T_N K	μ_{eff} μ_B	θ_p K
$NdIrIn_5$	4.648(3)	7.477(6)	161.53(4)	13.75	3.58(3)	≈18
Nd_2IrIn_8	4.647(3)	12.139(6)	262.14(3) [a]	12.30	3.60(3)	≈13
$NdRhIn_5$	4.630(3)	7.502(6)	160.82(4)	11	3.66(3)	≈17
Nd_2RhIn_8	4.640(3)	12.171(6)	262.04(3)	10.7	3.57(3)	≈14
$NdIn_3$	4.6530 [a]		100.74	≈6 [a]	3.62 [a]	≈17 [a]

[a]See Refs. 8–10.

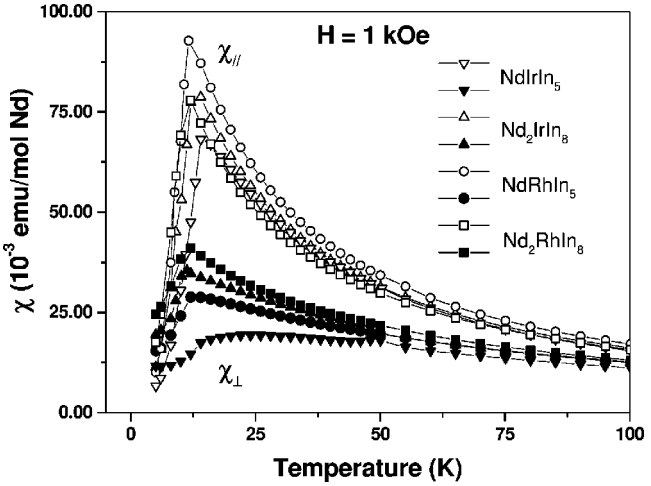

FIG. 1. Temperature dependence of the magnetic susceptibility, for applied field H along the c axis, $\chi_{\|}$ (open symbols), and in the ab plane, $\chi_{\perp}$ (solid symbols), for the studied $Nd_mM_nIn_{3m+2n}$ materials. The μ_{eff} and θ_p, obtained from Curie-Weiss law fitting for $T>150$ K using polycrystalline average of these data, are given in Table I.

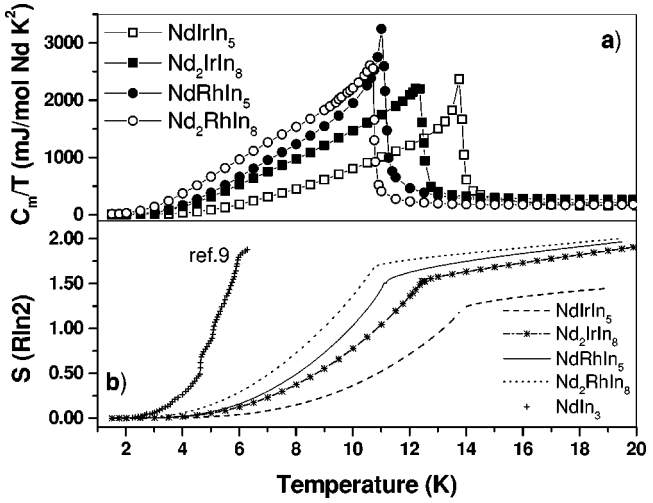

FIG. 2. The magnetic contribution to the specific heat divided by temperature (a) and the corresponding magnetic entropy (b) in the temperature range 2 K$\lesssim T\lesssim$20 K, for NdMIn$_5$ and Nd$_2M$In$_8$ (M=Rh or Ir).

III. RESULTS

Figure 1 presents the temperature dependence of the magnetic susceptibility, for an applied field H along the c axis, $\chi_{\|}$ and in the ab plane, $\chi_{\perp}$ for the $Nd_mM_nIn_{3m+2n}$ materials. Each shows antiferromagnetic order, with $T_N<14$ K. As might be expected from their quasi-2D structure, the magnetic susceptibility of these materials is anisotropic and depends on the value of m as well as the transition metal M. The ratio of $\chi_{\|}/\chi_{\perp}$ at T_N is larger for $m=1$ than for $m=2$, ranging from greater than 3 for $m=1$, M=Rh to 1.9 for $m=2$, M=Rh, and the ratio is always greater than one. The effective magnetic moment(μ_{eff}) and the paramagnetic Curie-Weiss temperatures (θ_p), obtained from Curie-Weiss law fits for $T>150$ K using polycrystalline average of these data, are given in Table 1.

Figure 2 shows the magnetic contribution to the specific heat divided by temperature [2(a)] and the corresponding magnetic entropy [2(b)] in the temperature range 2 K$\lesssim$T$\lesssim$20 K, for NdMIn$_5$ and Nd$_2M$In$_8$ (M=Rh or Ir). To obtain the magnetic contribution to the specific heat, the phonon contribution was subtracted from the original data using the specific heat data of LaMIn$_5$ and La$_2M$In$_8$ (M=Rh or Ir). The peaks in C_m/T corresponding to the onset of antiferromagnetic order can be seen at T_N=13.75, 12.30, 11.00, and 10.70 K for NdIrIn$_5$, Nd$_2$IrIn$_8$, NdRhIn$_5$, and Nd$_2$RhIn$_8$, respectively [Fig 2(a)]. The Néel temperatures obtained from the specific heat data are in very good agreement with the temperatures where the maximum in the magnetic susceptibility occurs (see Fig. 1). The magnetic entropy recovered by T_N ranges between 1.2-1.7R ln 2 [see Fig. 2(b)], suggesting that the magnetic order develops in a crystal field doublet groundstate with a nearby doublet excited state.

The temperature dependence of the normalized electrical resistivity for NdMIn$_5$ and Nd$_2M$In$_8$ (M=Rh or Ir) single crystals is plotted in Fig. 3. The room temperature value of the electrical resistivity varies between 10–30 $\mu\Omega$ cm and the high temperature data show a metallic behavior for these compounds. At low temperatures, clear features can be seen at the respective ordering temperatures for all compounds.

In Fig. 4 we replot the magnetic specific heat divided by temperature now as a function of T^2. The solid lines are the expected linear dependence for antiferromagnetic magnons at $T<T_N$. The inset presents the magnetic specific heat divided by temperature as a function of T^2 for Nd$_2$RhIn$_8$. The crosses in the inset represent a simulation of a crystal field Schottky anomaly[7] obtained from a doublet ground state with an excited doublet 20 K above. Subtracting this Schottky contribution from the Nd$_2$RhIn$_8$ specific heat data, we recover the expected linear behavior.

IV. DISCUSSION

The cubic compound NdIn$_3$ is an antiferromagnet with $T_N\approx 6$ K.[8,9] Magnetic order develops in a Γ_8 quartet crystal-field ground state with [001] being the easy axis.[9,10] Below T_N, additional magnetic transitions were observed. The re-

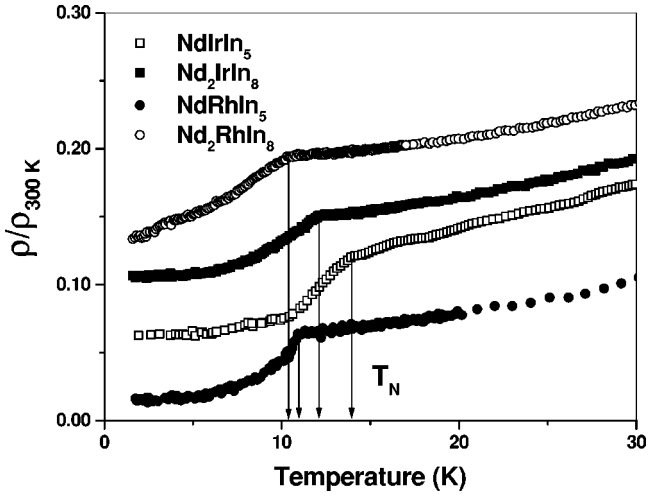

FIG. 3. Temperature dependence of the normalized electrical resistivity for NdMIn$_5$ and Nd$_2M$In$_8$ (M=Rh or Ir) single crystals.

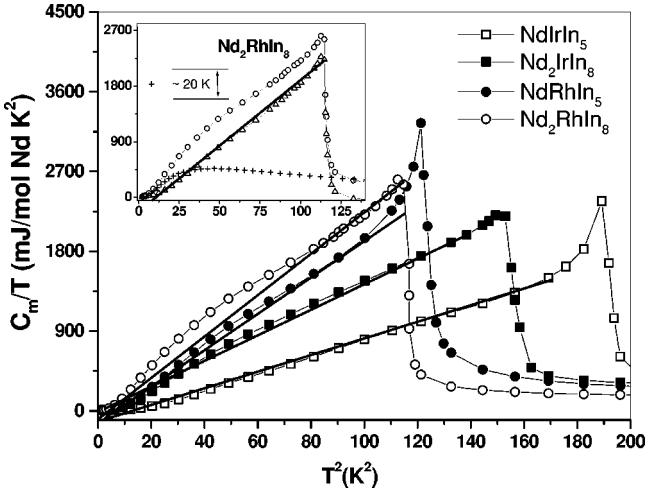

FIG. 4. Magnetic specific heat divided by temperature replotted as a function of T^2 for the data presented in Fig. 2. The solid lines are the expected linear dependence for antiferromagnetic magnons at $T<T_N$. The inset presents the magnetic specific heat divided by temperature as a function of T^2 for Nd_2RhIn_8. The crosses in the inset are the expected crystal field Schottky anomaly contribution due to a doublet ground state with an excited doublet ~20 K above.

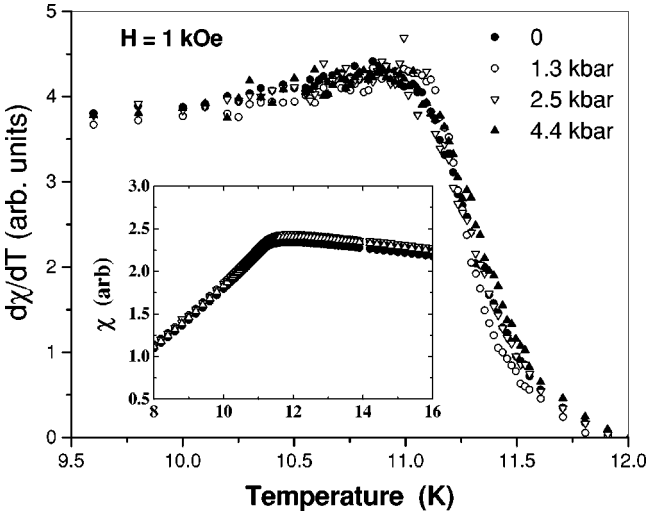

FIG. 5. Temperature and pressure dependence of the magnetic susceptibility derivative for $NdRhIn_5$ powdered crystals up to ≈4.5 kbar. The inset presents the original data from which the derivatives were taken.

sulting complex magnetic phase diagram with metamagnetic processes arises due to the presence of crystal field and magneto-elastic effects and both bilinear and quadrupolar exchange interactions.[9]

Surprisingly, the insertion of M-In layers along the c axis in $NdMIn_5$ and Nd_2MIn_8 (M=Rh or Ir) causes the Néel temperatures to increase by a factor of 2 (see Table I and Fig 6). Among the tetragonal variants, T_N is larger for Ir variants and for single layers variants. (see Table I and Fig. 6). No evidence for extra transitions below T_N was observed for the tetragonal compounds.

The simplest interpretation for the observed evolution of T_N among these Nd-based compounds would be a spatial dependence of the effective exchange parameter between Nd ions ($J_{\text{Nd-Nd}}$). The average distance between Nd ions, which can be deduced from the lattice parameters (Table I), can increase or decrease $J_{\text{Nd-Nd}}$ and consequently T_N. In this simple scenario, one can assume that $J_{\text{Nd-Nd}}$ is volume dependent and make the following estimate. The increase in volume for $NdIrIn_5$ compared to $NdRhIn_5$ is about 1 $Å^3$ and the difference between the T_Ns of these compounds is 2.75 K, with T_N larger for the compound with larger volume(see Table I and Fig. 6). A similar trend is also observed for the bilayer variants (see Table I and Fig. 6). Using a bulk modulus of ~1 Mbar,[11] a positive pressure of about 6 kbar is required to produce the difference in volume between $NdIrIn_5$ and $NdRhIn_5$. Thus, one should expect a pressure-induced evolution in T_N (dT_N/dP) of ≈ -0.5 K/kbar for $NdMIn_5$, assuming that the evolution of T_N is simply related to the change in lattice parameters. To test this supposition, pressure dependent magnetic susceptibility experiments were performed for $NdRhIn_5$ powdered crystals. The derivative of the magnetic susceptibility as a function of temperature for different applied pressures is shown in Fig. 5. The inset presents the original data from which the derivatives were taken. No appreciable changes in the Néel temperatures ($dT_N/dP \approx 0$) were observed up to ≈4.5 kbar for $NdRhIn_5$ (see Fig. 5) According to the ansatz above, a shift of about 2 K should have had been observed in this experiment. Thus, the evolution of T_N among these compounds cannot be explained by only a spatial dependence of $J_{\text{Nd-Nd}}$.

On the other hand, the evolution of T_N can be explained qualitatively by the character of the crystal field ground state

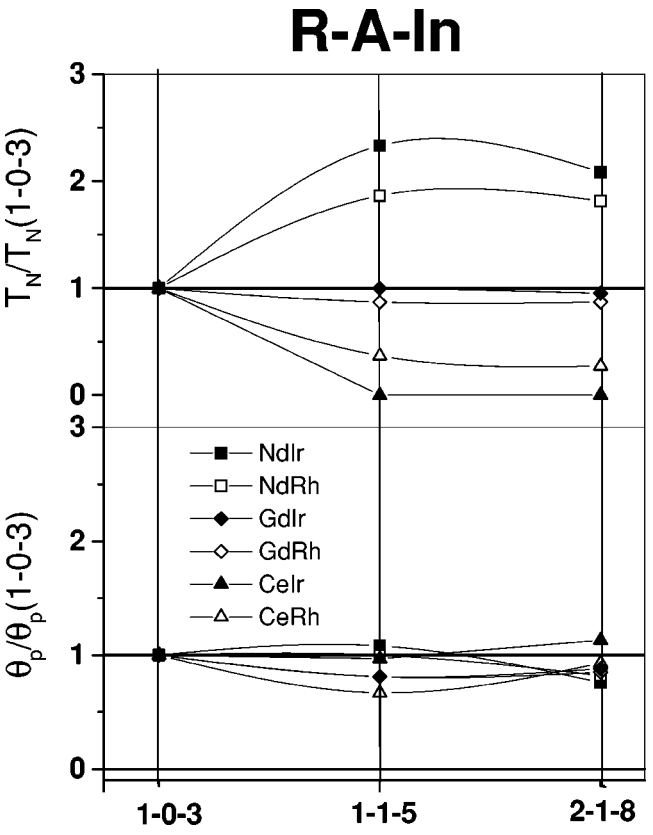

FIG. 6. Evolution of the normalized Néel and paramagnetic Curie-Weiss temperatures for the studied Nd-based compounds. For comparison, data for the homologous Ce- and Gd-based compounds and for cubic $CeIn_3$, $GdIn_3$, and $NdIn_3$ are also shown.

and the extent to which it is isolated. Figure 2(b) shows that $NdIrIn_5$ recovers the least magnetic entropy by $T=20$ K among the tetragonal variants, and the amount of entropy recovered by 20 K increases sequentially as $NdIrIn_5$-Nd_2IrIn_8-$NdRhIn_5$-Nd_2RhIn_8. Although specific heat data for $NdIn_3$ to $T=20$ K are not available, the recovered entropy at T_N and the Γ_8 quartet ground state suggest that the recovered entropy by 20 K would be even bigger for cubic $NdIn_3$ [see Fig. 2(a)]. Below, we argue that the fact that T_N decreases in the same sequence $NdIrIn_5$-Nd_2IrIn_8-$NdRhIn_5$-Nd_2RhIn_8-$NdIn_3$ is not accidental (see Table I).

Figure 4 shows a stronger deviation from the expected T^3 behavior ($T<T_N$) for those compounds in which more entropy is recovered, and the simulation presented in the inset of the figure suggests that the deviation is due to the population of a nearby excited crystal field doublet. In other words, $NdIrIn_5$, which recovers the least entropy by 20 K, has the more isolated crystal field doublet ground state and the largest T_N of the series. These results suggest that T_N is increased by the splitting of the Γ_8 quartet ground state into two doublets for the less symmetric variants and also that T_N increases with increasing doublet-doublet splitting.

The Nd^{3+} ($J=9/2$) ion in axial symmetry can have a very anisotropic (with its g value $g_{\|c} \gg g_{\perp}$) doublet as its ground state.[12] The interplay among interionic anisotropic exchange coupling, anisotropic CEF, and magnetocrystalline anisotropy can lead to frustration of the magnetic state at reduced ordering temperatures.[13–15]The reported anisotropic magnetic susceptibility data, the quasi-2D crystal structure of the tetragonal variants and the complex magnetic ordering state observed in $NdIn_3$ suggest that these effects may be present in the studied compounds (see Fig. 1 and Ref. 9). Further, it has been reported that $NdIn_3$ has [001] as an easy axis[9,10] and the tetragonal variants are also more susceptible for $H\|c$ (see Fig. 1), suggesting a [001] easy axis. Based on this scenario it is not unreasonable to suppose that the splitting of the Γ_8 quartet ground state into highly anisotropic doublets may decrease magnetic frustration, favoring order along the [001] direction at higher temperatures. Similar trends in low-temperature magnetic properties have been reported for other Nd-based compounds in tetragonal structures, for which competing CEF and magnetic anisotropies are present.[16–19]

Preliminaries studies in the Gd-based homologues $GdMIn_5$ and Gd_2MIn_8 ($M=$Rh or Ir) show antiferromagnetic ordering at about the same temperature as cubic $GdIn_3$ ($T_N \approx 45$ K)[8,1] for all tetragonal variants. (see Fig. 6) This absence of significant T_N evolution for the Gd-based compounds, for which CEF should be small due the S-ion character of Gd^{3+}, also suggest that observed T_N evolution for non-S rare-earth compounds might be CEF related. In addition, the CEF and the consequent low-temperature splitting should not be strongly affected by small values of pressure.[11] In this respect, no significant T_N pressure dependence should be expected for these Nd-based compounds in the scenario above, which agrees with the Fig. 5 data for $NdRhIn_5$. Further CEF studies and investigation of the character of the magnetic state for $NdMIn_5$ and Nd_2MIn_8 ($M=$Rh or Ir) by neutron scattering and/or magnetic resonance techniques (NMR,ESR,NQR) would be valuable in confirming our supposition.

Finally, to compare $R=$Ce, Nd, and Gd materials, Fig. 6 shows the evolution of the Néel temperature and the paramagnetic Curie-Weiss temperatures for the homologous $RMIn_5$ and R_2MIn_8 ($R=$Nd, Ce,Gd, $T=$Rh or Ir) compounds compared to the their cubic RIn_3 (Nd,Ce,Gd) relatives. As one can see, θ_p shows little change among these series for $R=$Nd, Ce, and Gd. The result indicates that in the molecular field approximation, the effective exchange parameter between rare-earths remains about the same at high temperatures through these homologous series for $R=$Nd, Ce, and Gd. On the other hand, T_N shows significant evolution for the non-S $R=$Nd and Ce materials, suggesting again that the low-temperature crystal field configuration is an important contribution to the observed evolution. Further, the T_N evolution for $R=$Nd and Ce based compounds appears to be qualitatively similar, but occurring in opposite directions (see Fig. 6). T_N is raised by a factor 2 for the Nd-based tetragonal variants and is suppressed completely ($M=$Ir) or to less than 0.5 of the $CeIn_3$ value ($M=$Rh) for the Ce-based homologous compounds.[2–5] The $M=$Ir versions have the largest T_N values for the Nd-based compounds and are the ones where the magnetism is totally suppressed in the Ce case.[2–5] As was discussed above, the T_N evolution for the Nd-based compounds, for which Kondo effects are not present, can be qualitatively explained by a crystal field induced enhancement in $J_{\text{Nd-Nd}}$ among these compounds. Based on the similarities with the Nd case (see Fig. 6) it is not unreasonable to suppose that similar CEF can interfere in the interplay between the Kondo effects and the RKKY magnetic interaction driving different ground states for these new heavy fermion Ce-based compounds. Similar competing CEF and magnetic exchange anisotropies drive non-Doniach-like phase diagrams for other heavy fermion compounds such as YbNiSn and YbPtAl.[13,14]

V. CONCLUSIONS

We have reported a new series of Nd-based antiferromagnetic compounds. The evolution of their magnetic properties depends on the crystal-field ground-state configuration. The observed evolution appears to be related to the symmetry of the crystal-field ground state and how isolated it is. Our results suggest that a splitting of the Γ_8 quartet ground state to highly anisotropic doublets for the tetragonal $NdMIn_5$ and Nd_2MIn_8 ($M=$Rh or Ir) compounds decreases magnetic frustration, favoring order along the [001] direction at higher temperatures. Similarities between the present data and magnetic properties of the isostrucutural new heavy fermion materials (HFS) $Ce(Rh,Ir)In_5$, $Ce_2(Rh,Ir)In_8$ suggest that CEF and magnetic anisotropy investigations for $CeMIn_5$ and Ce_2MIn_8 ($M=$Rh or Ir) by neutron scattering and/or magnetic resonance techniques (NMR,ESR,NQR) are needed to fully understand the rich phase diagram of these compounds.

ACKNOWLEDGMENTS

We thank Z. Fisk and S.B. Oseroff for helpful discussions. Work at Los Alamos was performed under the auspices of the U.S. Dept. of Energy. P.G.P. also thanks FAPESP (SP-Brazil) Grant No. 99/01062-0.

[1] P.G. Pagliuso, M.F. Hundley, J.D. Thompson, J.L. Sarrao, Z. Fisk, G.B. Martins, S.B. Oseroff, R. Urbano, H. Martinho, and C. Rettori (unpublished).
[2] H. Hegger, C. Petrovic, E.G. Moshopoulou, M.F. Hundley, J.L. Sarrao, Z. Fisk, and J.D. Thompson, Phys. Rev. Lett. **84**, 4986 (2000).
[3] C. Petrovic, R. Movshovich, M. Jaime, M.F. Hundley, J.L. Sarrao, P.G. Pagliuso, Z. Fisk, and J.D. Thompson (unpublished).
[4] J.D. Thompson, R. Movshovich, Z. Fisk, F. Bouquet, N.J. Curro, R.A. Fisher, P.C. Hammel, H. Hegger, M.F. Hundley, M. Jaime, P.G. Pagliuso, C. Petrovic, N.E. Phillips, and J.L. Sarrao, J. Magn. Magn. Mater. (to be published)
[5] R. Movshovich, C. Petrovic, M. Jaime, M.F. Hundley, J.L. Sarrao, Z. Fisk, P.G. Pagliuso, and J.D. Thompson (unpublished).
[6] R. Bachmann, F.J. DiSalvo, T.H. Geballe, R.L. Greene, R.E. Howard, C.N. King, H.C. Kivisch, K.N. Lee, R.E. Schwall, H.V. Thomas, and R.B. Zubek, Rev. Sci. Instrum. **43**, 205 (1972).
[7] See, for example, E.S.R. Gopal, *Specific Heat at Low Temperatures* (Plenum Press, New York, 1966).
[8] K.H.J. Buschov, H.W. de Wijn, and M. Van Diepen, J. Chem. Phys. **50**, 137 (1969).
[9] M. Amara, R.M. Galéra, P. Morin, T. Verez, and P. Burlet, J. Magn. Magn. Mater. **130**, 127 (1994); M. Amara, R.M. Galéra, P. Morin, J. Voiron, and P. Burlet, *ibid.* **131**, 402 (1994); **140-144**, 1157 (1994).
[10] A. Czopnik, J. Kowalewski, and M. Hackemer, Phys. Status Solidi A **127**, 243 (1991).
[11] J.D. Thompson and J.M. Lawrence, in *Handbook on the Physics and Chemistry of Rare Earths*, edited by K.A Gscneider, Jr. *et al.* (Elsevier, Amsterdam, 1994) Vol. 19, p. 383.
[12] A. Abragam and B. Bleaney, *Electron Paramagnetic Resonance of Transition Ions* (Clarendon, Oxford, 1970).
[13] K. Drescher, M.M. Abd-Emeguid, H. Micklitz, J.P. Sanchez, C. Geibel, and F. Steglich, J. Magn. Magn. Mater. **182**, L275 (1998).
[14] K. Drescher, M.M. Abd-Emeguid, H. Micklitz, and J.P. Sanchez, Phys. Rev. Lett. **77**, 3228 (1996).
[15] P. Bonville, P. Bellot, J.A. Hodges, P. Imbert, G. Jéhanno, G. Le Bras, J. Hammann, G. Chevrier, P. Thuéry, L.D. D'Onofrio, A. Hanzi, and A. Barthélémy, Physica B **182**, 105 (1992).
[16] W. Henggeler, T. Chattopadhyay, B. Roessli, D.I. Zhigunov, and A. Furrer, Z. Phys. B **99**, 465 (1996).
[17] F. Fourgeot, B. Chevalier, D. Laffargue, and J. Etourneau, J. Magn. Magn. Mater. **182**, 124 (1998).
[18] A.N. Bazhan, J. Magn. Magn. Mater. **185**, 228 (1998).
[19] D. Givord, H.S. Li, and F. Tasset, J. Appl. Phys. **57**, 4100 (1985).